Vol. 41, No. 3 (2019) 375-386, DOI: 10.24874/ti.2019.41.03.07

Tribology in Industry

www.tribology.rs

RESEARCH

Study of Mechanical and Sliding Wear Behavior of Al-25Zn alloy/SiC/Graphite Novel Hybrid Composites for Plain Bearing Application

P.P. Ritapure[a,b], Y.R. Kharde[c]

[a]*Zeal College of Engineering and Research, Pune-411041, Maharashtra, India,*
[b]*Amrutvahini College of Engineering, Sangamner-422605, Maharashtra, India,*
[c]*Pravara Rural Engineering College, Ahmednager-413736, Maharashtra, India.*

Keywords:

Sliding wear
Hybrid composites
Surface morphology
Aluminium-zinc alloy
Temperature
Artificial neural network

Corresponding author:

Parmeshwar P. Ritapure
Zeal College of Engineering and Research, Pune-411041, Maharashtra, India.
Amrutvahini College of Engineering, Sangamner-422605, Maharashtra, India.
E-mail: ritapurep@yahoo.co.in

A B S T R A C T

In this investigations, sliding wear performance of Al-25Zn based novel hybrid composites added with fixed weight percentage of graphite (3 wt.%) and varying weight percentage of silicon carbide (10, 20 and 30 wt.%) was investigated for various process factors such as specimen temperature, applied load, sliding speed and sliding distance using a pin on disc with EN24 disc as per Taguchi L_{16} array. For similar test conditions, the composite with 10 wt.% of silicon carbide shows the highest wear resistance and tensile strength; whereas the composite with 20 wt.% of SiC shows highest hardness. The specimen temperature is recognized as the dominating parameter for the sliding wear performance of the materials. Artificial Neural network and Regression model developed was found competent for the forecasting of wear performance. Confirmation experiment conducted with the optimum parameter combination also confirmed the accuracy of developed model. The observed wear mechanism is abrasion and adhesion. The major mechanisms of abrasive wear are recognized as ploughing, micro cutting and delamination.

1. INTRODUCTION

Metal matrix composites based on aluminum Zinc alloy are presently finding better utility in various engineering applications due to excellent sliding wear and mechanical characteristics. Among zinc aluminum (ZA) alloy family ZA-27 is the strongest and commonly used material for bushing, plain bearing and many sliding wear application. In automobile industry, mechanical press, compressors, hydraulic, steam and gas turbines, gear pumps etc. plain bearing is commonly used [1-4]. ZA alloys are observed as the excellent bearing

materials as that of current materials like bronze brass, [1], bearing alloy [2] copper base alloy [3], cast iron [6] and SAE 65 bronze [7] owing to better wear resistance, high fatigue and tensile strength, small coefficient of friction, high hardness, light in weight, excellent load carrying capacity and corrosion resistance. However, these alloys suffer from some drawback like dimensional instability, small impact strength and ductility and poor performance at elevated temperature limits application of these alloys [5,8,28]. These drawbacks are reduced to certain extent by increasing share of aluminum as compared with zinc in alloy [10-17]. Aluminium alloys with 19 to 27 wt.% zinc are beneficial bearing alloy and used for different vehicle parts that demands self-lubrications and wear resistance [11-12]. These alloys have outstanding fatigue strength and hence used for sliding bearing situations [13]. Al-25Zn, Al-25Zn-3Cu, Al40Zn3Cu2.5Si and Al40Zn3Cu shown better ductility, strength, hardness and wear resistance that of ZA alloy, SAE 65 bronze and bearing bronze [9,10,13-17].

Tribological and mechanical characteristics of ZA alloys were enhanced by addition of zircon [18], garnet [19], glass fiber [20-22], Al_2O_3 [23], Titanium-Dioxide [24], TiC [25], graphite [26-29] and SiC. Graphite particle addition into ZA alloys significantly enhance ductility tensile and compressive strength, and Young's modulus, but reduce the hardness of metal matrix composite. Graphite reinforced ZA alloy based composite found significant application in engine bearing, cylinder liners, engine block, cylinder heads and liners, piston and piston rings [26-29]. Addition of SiC into ZA alloy enhances the tribological and mechanical behavior except reduction in impact strength and ductility. SiC reinforced composites are commonly employed for different application like engine bearing, brake drum and rotor, driveshaft, piston and piston rings and engine tail guide vanes [30-35].

Rao and Das [33] found reduction in wear rate with addition of SiC in various aluminum alloys. Ghosh and Saha [34] suggested that the addition of SiC above 15 vol.% is not beneficial as crack density and wear rate reduces rapidly. Thella Babu Rao [35] noticed that addition of SiC reduces impact strength and ductility of aluminum composite.

The reinforcement of 3 wt.% of graphite in Al-25Zn alloy enhances the wear resistance and tensile strength of composite, in spite of the substantial drop in hardness. The rise in strength and drop in hardness by substantial amount is noticed with increase of graphite reinforcement from 0 % to 5 % in a step of 1 wt.%. However, the highest wear resistance is noticed for the materials with 3 wt.% of graphite [45]. Hence fixed 3 wt.% of graphite was selected as reinforcement into matrix alloy.

The novelty of research includes i) the intention of this research was to know the effect of constant 3 wt.% of graphite addition into Al-25Zn alloy with the various weight percentage of SiC on tribological and mechanical behavior of the hybrid composite to identify better option for existing bearing material and similar application of wear resistance. Therefore the objective of this experimental work was to optimize SiC contents in Al-25Zn alloy in presence of 3 wt.% of graphite.

The influence of specimen temperature on sliding wear performance of Al-25Zn composite is hardly seen in the reported literature [11-17]. In the present research different process factors including specimen temperature have been optimized for wear resistance by using Artificial Neural network (ANN) and design of the experiment [36-39].

2. MATERIAL AND EXPERIMENTAL METHOD

2.1 Fabrication of composites

Four materials of chemical composition in different weight percentage given in Table 1 were manufactured by stir casting.

Table 1. Composition and porosity in composites.

Composition (weight percentage)	Theoretical Density (kg/m^3)	Experimental Density (kg/m^3)	Porosity (%)
Al25Zn3Gr	3165.45	3109±4	1.82
Al25Zn3Gr10SiC	3169.85	3117±6	1.66
Al25Zn3Gr20SiC	3174.26	3061±9	3.56
Al25Zn3Gr30SiC	3178.68	3054±11	3.92

The matrix alloy selected Al-25Zn was prepared from Zinc and aluminum ingots of

purity 99.9 % supplied by Parshwamani Metals. Graphite and SiC particles of approximately size of 25 μm supplied by Sunshree traders were used as reinforcement. Zinc and aluminum ingots were cut into small parts and added into 4 kg capacity graphite crucible and heated for the 700 ^{0}C temperature. To reduce porosity the melt was further heated by 100 ^{0}C and kept at same temperature for half hour. To boost the wettability, 1 wt.% magnesium was added into the melt. The mixture of Aluminium, graphite and magnesium forms compounds which provides the strength to composite [40,41]. Simultaneously graphite and SiC particles were heated to in other furnace to 450 ^{0}C and 500 ^{0}C respectively to improve thermal solidity and to reduce moisture. Mechanical stirrer with speed 500 rpm used for stirring of melt and then preheated graphite and SiC particles added into vortex developed due to stirring. Stirring process further continued for 5-7 minute still even distribution was achieved. To remove the entrapped gases from the melt tablets of Hexachloroethane ethane were added and then melt was poured into preheated die (mild steel) of 20mm diameter and 300 mm length. After complete solidification at ambient conditions, specimens were taken out from die.

2.2 Density and Porosity

Archimedes' principle with ethanol medium was used to measure the experimental density (ρ) of manufactured materials [46]. Average of seven observations recorded gives the experimental density for individual material. Theoretical density is calculated from rule of mixture. The amount of porosity in the fabricated material shown in Table 1 is determined from the Eq. (1) shown below:

$$\%\ Porosity = \left(\frac{\rho_{Theoretical} - \rho_{Experimental}}{\rho_{Theoretical}}\right) \times 100 \quad (1)$$

2.3 Tensile testing

Universal Testing machine (Instron 1195) was used to measure the tensile strength of manufactured materials following ASTM E8 standard at 32 ^{o}C temperature with maximum 400N load and 8.3×10^{-5} m/s speed of crosshead. Average of three test replications gives the value of strength for individual material.

2.4 Hardness measurement

Brinell hardness tester (model B 3000) was used to measure the hardness of materials following ASTM E10 standards at 32 ^{o}C temperature with 5 mm ball indenter. Average of five replications gives the hardness for each material.

2.5 Surface Morphology

The surface morphology of the worn surfaces of composites were examined using Scanning Electron Microscope (SEM), model Nova Nano SEM-450, FEI make. The samples used for SEM examination of dimension 8×8×4 mm were cut from the worn out specimens. Before SEM examination samples were polished with platinum paste using polishing machine and cleaned with ethanol.

2.6 Sliding wear test

Pin on disc universal tribometer, Ducom make, Bangalore was used for wear test. The un-lubricated tests were executed following ASTM G-99-95a standard for the selected factors presented in Table 2.

Table 2. Control parameters and their Levels.

Control Parameters	Level				Units
	I	II	III	IV	
Sliding Speed (A)	1	2	3	4	m/s
Load (B)	20	40	60	80	N
Temperature (C)	40	60	80	100	^{o}C
Sliding Distance (D)	1.57	3.5	4.54	5.5	km
Filler content (E)	0	10	20	30	wt.%

The specimen used of diameter 12 mm and 30 mm length. Wear is a complex phenomenon; hence test outcome depends on behavior of counterpart. The disc material selected was EN-24 (shaft steel) of surface roughness 0.5 μm and hardness of 50 HRC. EN24 or EN8 shaft steel and aluminium based bearing alloy is commonly used tribo-pair for plain bearing applications. EN 24 steel has good ductility, high tensile strength, high shock resistance, more hardness and high wear resistance as that of EN 8 steel [42]. The liquid nitride EN 24 is harder than EN31 steel [43]. The EN 24 is shaft steel and commonly employed for stressed situations like camshaft, connecting rod, spindles, rotor shaft, crankshaft, gear shaft and for similar engineering application.

To obtained accurate results wear tests were repeated thrice and average of wear rate in micron calculated from Eq. (2) is shown in Table 3.

$$\text{Wear rate} = \frac{\left(Initial\,mass\,loss - final\,mass\,loss\right)}{density} \quad (2)$$

Table 3. Wear results as per L_{16} (4^5).

Test	A	B	C	D	E	Wear	SN ratio
1	1	20	40	1.57	0	175	-44.9
2	1	40	60	3.52	10	262	-48.4
3	1	60	80	4.54	20	338	-50.6
4	1	80	100	5.5	30	425	-52.6
5	2	20	60	4.54	30	270	-48.6
6	2	40	40	5.5	20	232	-47.3
7	2	60	100	1.57	10	390	-51.8
8	2	80	80	3.52	0	428	-52.6
9	3	20	80	5.5	10	339	-50.6
10	3	40	100	4.54	0	437	-52.8
11	3	60	40	3.52	30	302	-49.6
12	3	80	60	1.57	20	403	-52.1
13	4	20	100	3.52	20	396	-52.0
14	4	40	80	1.57	30	380	-51.6
15	4	60	60	5.5	0	419	-52.4
16	4	80	40	4.54	10	361	-51.2

2.7 Selection of factors and their level

The selection of levels for parameters shown in Table 2 was done on the basis of i) by referring available literature [1-10, 13-35] ii) from the trial tests conducted for the variety of parameters available on setup.

a) The range of sliding speed was selected from 1 m/s to 4 m/s and middle speeds were determined using arithmetic progression. Trial tests were executed for different velocities by altering test duration, track diameter and/or speed in rpm. For fixed track diameter test duration turn out to be extremely small at very high speed and vice versa. The variations in the tests results from the repetitive test for the speeds selected outside range was from 9 to 14 %, where as for the speed range 1-4 m/s is 0.5 to 1 %.

b) The range of applied load was selected from 20 N to 80 N. It was observed for the load selected beyond 80 N that i) cracking of SiC particles leads to fracture ii) the soft graphite particles squeezing out very rapidly. The wear rate noticed almost same for all the composites for load less than 20 N.

c) The range of pin temperature was selected from 40 to 100 ^{0}C. The room temperature varies with seasons as well as time and hence to maintain uniformity 40 ^{0}C temperature was selected. However, it was noticed for the temperature selected above 115-120 ^{0}C, specimen becomes very soft and hence asperities on disc penetrated the specimen and there was a formation and breaking of cold weld junction at contact leads to sever wear of the composites and then we must to conclude the test before planned sliding distance.

2.8 Design of Experiment

The wear tests were performed following Taguchi array $L_{16}4^5$. Wear results were analyzed using MINITAB 17 with governing criteria as signal to noise (S/N) ratio. The purpose of this work was to obtain minimum wear rate and hence S/N ratio approach "smaller-the-better" was considered.

$$\frac{S}{N} = -10 \times \log\left(\frac{\Sigma\left(Y^2\right)}{n}\right) \quad (3)$$

Where Y = responses (wear value obtained for test run) and n = total number of responses [44].

2.9 ANN for prediction of wear rate

ANN has been implemented now days in different engineering application including Tribology and material science to forecast the relationship between process parameters and material characteristics. ANN is motivated from the functioning of human brain and it is based on database training. In this work ANN is successfully used to predict sliding wear behavior of composite for selected parameters as shown in Table 2.

ANN Multilayer Perceptron (MLP) comprises a large number of neurons (processing elements), which are arranged in different layers of the network such as an input layer, some hidden layers, and an output layer. The weights are assigned to the neurons [39]. The performance of developed network is depends on number of hidden layers and neurons in each hidden layers. The number of hidden layers was selected by trial and error process. The parameters

presented in Table 2 were selected as input layer neurons, these parameters were analyzed in the hidden layer and forecasting of wear rate is done at output layer. For network training 75 % of total data and for testing 25 % of total data were used to develop ANN model [36-39].

3. RESULTS AND DISCUSSION

3.1 Porosity

For the application which demands high fatigue and tensile strengths, the composites should have least or even no porosity [46-50]. Column 4 of Table 1 shows that the minimum porosity is noticed for the material with 10 wt.% of SiC, where as it increases slightly for the composite with 20 and 30 wt.% of SiC. Theoretical density is improved with the SiC particles addition for all the fabricated composites. The experimental density is increased for the composite with 10 wt.% of SiC, where as it reduces slightly for the composite with 20 and 30 wt.% of SiC. This reduction in experimental density is due to the development of entrapped gases during stir casting process with addition of SiC particles beyond certain limit. The least porosity for the material with 10 wt.% of SiC confirms outstanding bonding strength and chemical solubility among SiC, graphite and matrix alloy.

3.2 Tensile strength

Figure 1 show that maximum strength is noticed for the material having 10 wt.% of SiC. However reduction in strength noticed for the material with 20 and 30 wt.% of SiC.

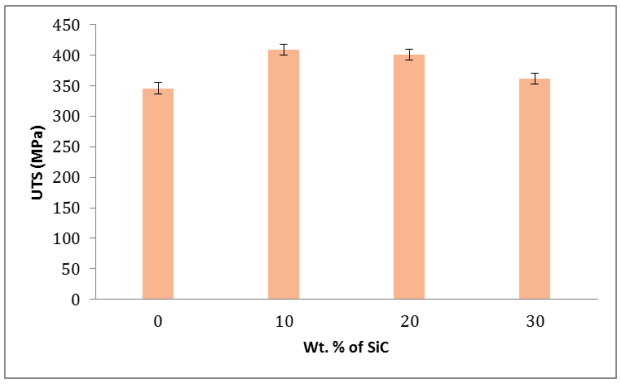

Fig. 1. Effect of SiC addition on tensile strength.

Figure 1 shows that tensile strength of base alloy improved with addition of soft graphite and strong SiC particles. The hard SiC particles takes maximum load and act as barrier for plastic flow [30-35]. Least porosity and more strength is noticed for the material having 10 wt.% of SiC indicates outstanding bonding strength and chemical solubility among SiC, graphite and matrix alloy. However strength and solubility decreases with further addition of SiC [26-29, 45].

3.3 Hardness

Figure 2 shows that the highest value of hardness is noticed for the material with 20 wt.% of SiC. With increase in SiC content from 0 wt.% to 20 wt.%, the hardness is increased by about 34 to 37 %.

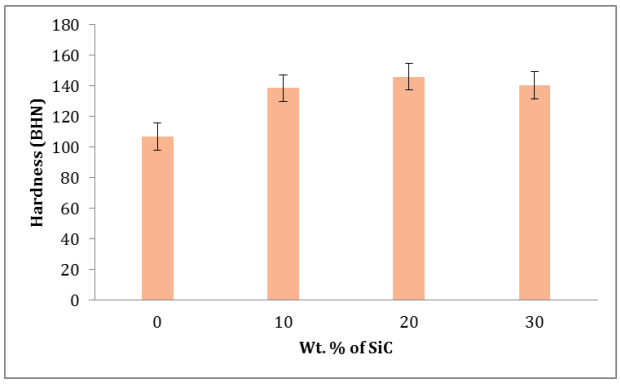

Fig. 2. Effect of SiC addition on Hardness.

However the hardness decreases slightly with further addition of SiC particles from 20 wt.% to 30 wt.%. This reduction in hardness may be due to the softness of graphite, as the graphite particulate being softer, hence does not act as obstacles to movement of displacements within the matrix [26-29,45] and reduction in strength and solubility decreases with further addition of SiC.

3.4 Effect of parameters on Wear rate

On execution of wear tests average wear rate values are shown in Table 3. Analysis of these results was carried out by MINITAB 17.

Figures 3-4 shows that the more powerful parameter for the wear rate of composite is temperature and then in sequence load, velocity, reinforcement quantity and sliding distance. This influence of parameters can be confirmed from the Δ (delta) value and rank as given in Tables 4-5 [44]. From Tables 4-5 it is noticed that the temperature is at rank 1, load at 2,

speed at 3, reinforcement at 4 and sliding distance at 5. The delta value is calculated from difference in higher and lower S/N ratio. The parameter having grater the values of delta is identified as most influencing parameter.

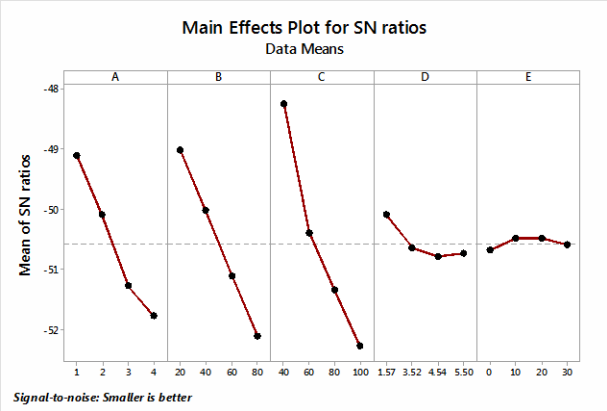

Fig. 3. Main effect plots for SN ratios.

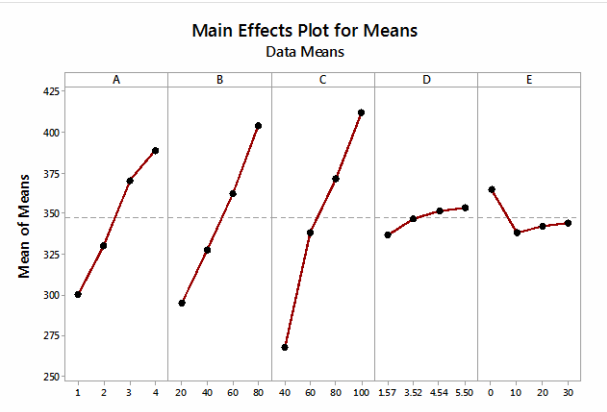

Fig. 4. Main effect plots for Mean.

Table 4. Response for Signal to Noise Ratios.

Level	A	B	C	D	E
1	-49.09	-49.01	-48.23	-50.1	-50.6
2	-50.1	-50.02	-50.39	-50.6	-50.4
3	-51.28	-51.11	-51.35	-50.7	-50.4
4	-51.79	-52.11	-52.29	-50.7	-50.6
Delta	2.69	3.1	4.06	0.7	0.2
Rank	3	2	1	4	5

Table 5. Response for Means.

Level	A	B	C	D	E
1	300	295	267.5	337	364.8
2	330	327.8	338.5	347	338
3	370.3	362.3	371.3	351.5	342.3
4	389	404.3	412	353.8	344.3
Delta	89	109.3	144.5	16.8	26.8
Rank	3	2	1	5	4

The parameter combination for maximum wear resistance observed from Figs. 3-4 is ($A_1B_1C_1D_1E_2$). The maximum wear resistance by all the material is observed at speed 1m/s, temperature 40 ^{0}C, load 20 N, sliding distance 1.57 km and composite with 10wt.%SiC.

Figures 3-4, shows that the wear resistance decreases with rise in temperature, loads, speed and distance. However least wear loss is noticed for the material with 10wt.%SiC. As temperature increases composites pin becomes soft and it may get ploughed by the asperities present on EN24 disc that leads to severe wear due to delamination and abrasion. With the rise in applied pressure, plastic deformation at asperity contact occurs that leads to building and breaking of cold weld junction results into detachment of free debris from specimen and/or its attachment to disc. The development of surface cracks and their subsequent fusion by shear deformation with rise in speed results into wear of the composite.

3.5 Analysis of variance

To know statistical implication and individual involvement of factors on sliding wear rate of the material analysis of variance (ANOVA) was executed at confidence level of 95 %. The significance of individual factors is decided from the p values shown in Table 6.

Table 6. ANOVA table for wear rate.

Source	DF	SS	F Value	p-value	% Con--tribution
Model	*5*	89908	63.7	*0.000*	*96.95*
A	1	18880	66.88	0.000	20.36
B	1	26245	92.97	0.000	28.30
C	1	43477	154.0	0.000	46.88
D	1	649.6	2.3	0.16	0.700
E	1	655.5	2.32	0.159	0.706
Error	10	2823			3.044
Total	15	92731			100

If p value for corresponding factors is less than 0.05 then that factor is considered as significant [44]. Table 6 shows that p value for temperature, load and sliding speed is small hence they have significantly contributed to wear of materials. The individual contribution of factors in

percentage presented in Table 6 validate the temperature is major contributing factor with of 46.88 %, followed by load (28.30 %), sliding speed (20.36 %), percentage reinforcement (0.706 %) and sliding distance (0.7 %). (F-Fisher test; SS-Sum of Squares).

3.6 Regression

The relationship between input parameters and response is derived by regression analysis as shown below in Eq. [4].

$$Wear = 8.8 + 30.7A + 1.8B + 2.3C + 4.3D - 0.57E \quad (4)$$

The positive coefficient of corresponding factors shows rise in wear loss; however negative coefficient shows to reduction in wear loss.

The value for coefficient of determination (R^2) close to 1 indicates the integrity of the regression model [44]. The R^2 96.95 and adjusted R^2=95.39 indicates that more than 95 % of variance is explained by regression model.

3.7 Confirmation experiment

This is the concluding step in the DOE to validate conclusions from experimental result analysis. The experiment was performed for optimal parameters ($A_1B1C_1D_1E_2$) and results are presented in Table 7. S/N ratio α for optimal factors can be calculated as:

$$\alpha = \alpha_m + \sum_{j=1}^{n} \left(\alpha_j - \alpha_m \right) \quad (5)$$

Where α_m- overall mean of the S/N ratio, n-number of factors and α_j- S/N ratio mean at the optimal level.

Table 7. Confirmation test results.

	Initial parameters	Optimal parameter		
		Prediction	Experiment	Error
level	$A_1B_1C_1D_1E_1$	$A_1B_1C_1D_1E_2$	$A_1B_1C_1D_1E_2$	
Wear	175	167	158	5.38
SN ratio	-44.87	-44.45	-43.95	

The error (5.38 %) in predicted and experimental wear value shown in Table 7 validate that the derived model is precisely capable for forecasting the wear characteristics of material.

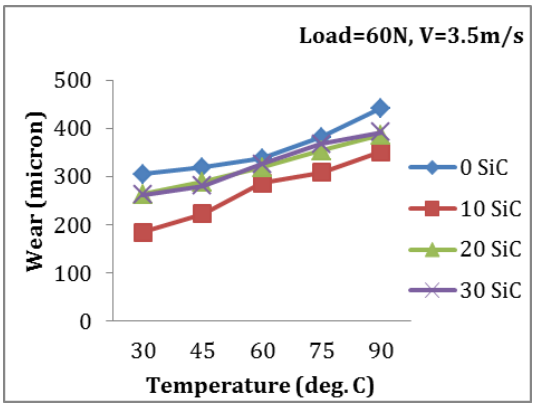

Fig. 5. Effect of pin temperature on wear rate.

Few additional experiments were performed to confirm the supremacy of temperature on wear resistance of material and results presented in Fig. 5 shows that for equal test condition material with 10 wt.% of SiC reveal excellent wear resistance.

3.8 Surface Morphology

Microstructure characterization of worn surface is essential to understand the wear mechanism [46-50]. Scanning Electron Microscope was used to examine worn surface for test conditions 4, 7, 10 and 12 (Table 3) as shown in Figs. 6a-6d.

Energy dispersive X-ray spectroscopy (EDS) micrographs of the material with 10 wt.% of SiC presented in Fig. 7 confirms the existence of matrix and reinforcement.

Rubbing of pin over disc at different operating condition leads to the plastic deformation of the specimen and hence soft graphite may squeeze out from the composite and form the film over the surface. Due to the lubricating properties of graphite, a film formed may act as a lubricant and reduces the direct contact of the specimen pin with disc during dry sliding wear test. Black layer over all the worn surfaces confirms the formation of black graphite solid film (Figs. 6a-6d) [26-29, 45].

The abrasion, adhesion and delamination wear mechanism is noticed over SEM micrographs. Scratches and grooves are observed due to ploughing and cutting. Figure 6b shows narrow and shallow groove above the worn surface of material with 10 wt.% of SiC. Whereas, increase in width and depth of grooves is noticed for the material with 20 and 30 wt.% of SiC (Figs. 6c-6d).

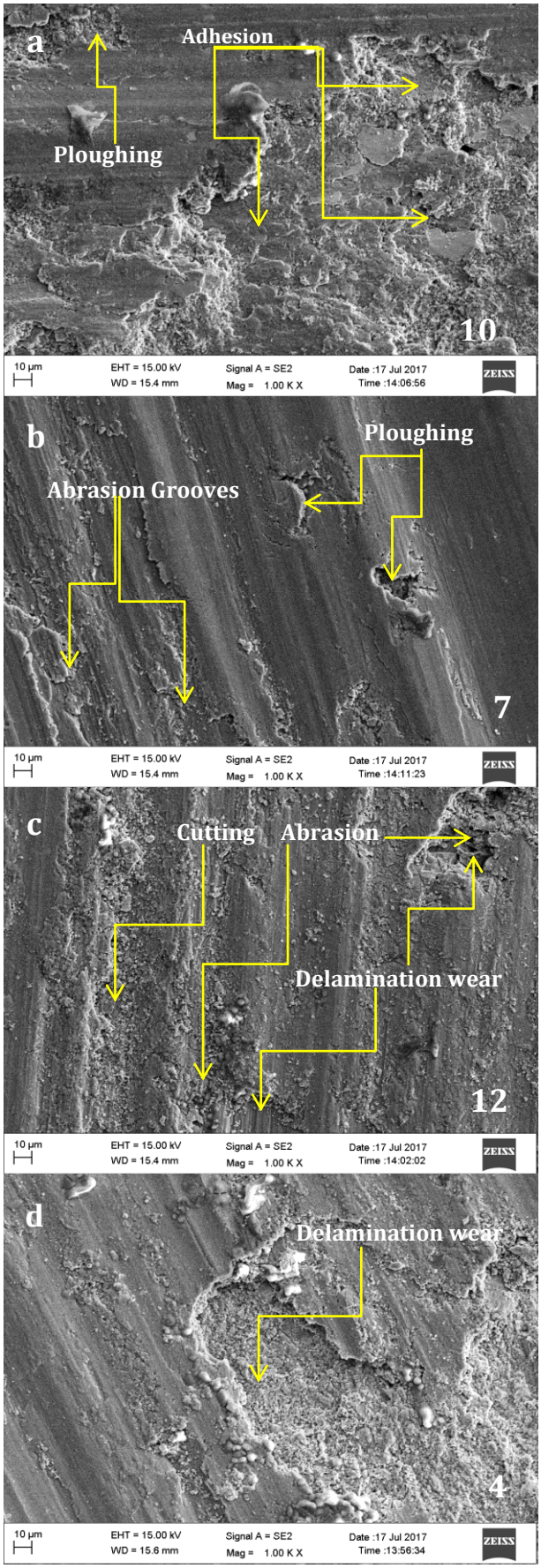

Fig. 6 (a-d). SEM micrographs of test conditions 4, 7, 10 and 12 (refer Table 3).

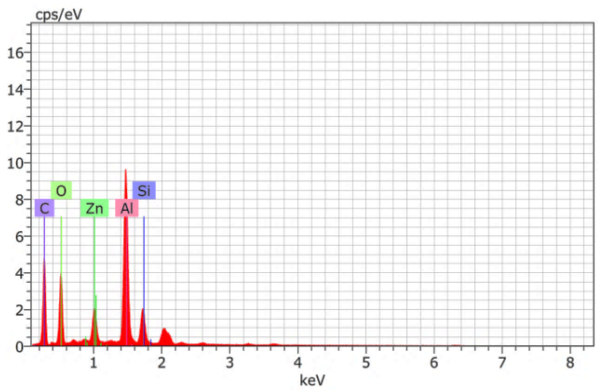

Fig. 7. EDS analysis for composite with 10%SiC.

Addition of SiC into Al25Zn alloy improves hardness, tensile strength and hence enhancement in wear resistance due to adhesion; however presence of harder and stronger SiC particles may cause wear due to delamination and abrasion. Figure 6a shows the wide and fine deep grooves over worn surface of the matrix alloy. A matrix alloy has less strength and hardness as that of composites and hence at high operating situation sliding wear occurs due adhesion. Also as matrix alloy being soft, asperities on steel disc may plough the matrix alloy that leads to wear due to abrasion.

SEM micrographs shown in Fig. 6 confirmed the influence of temperature, load and SiC addition on wear performance of the material. For all the operating conditions material with 10 wt.% of SiC shown least wear rate, maximum hardness and strength, hence less scratches and/or grooves seen over the surface. Due to delamination wear, large and fine deep grooves are seen in Fig. 6d for the material with 30 wt.% of SiC confirmed the weak bonding strength and solubility and this limits the addition of SiC beyond certain limit. For the high value of operating parameters material with 0, 20 and 30 wt.% of SiC experience severe wear. Whereas the material with 10 wt.% of SiC undergoes mild wear.

3.9 ANN model and Regression model

Several ANN models were tested by for different values of governing factors and 4-8-1 topology selected as per the smallest error criteria [36-39]. Remaining unused 25 % data was used for the evaluation of developed ANN model. Figure 8 shows that the developed models are precise for the forecasting of wear characteristics of the manufactured materials as the variation in wear

values predicted by regression model (R), ANN model (N) and experiment (E) is very small. The value of R^2 for regression model is 96.95 and for ANN model is 99.32 approves the good covenant between the models. The ANN model can be made more accurate further by enhancing the neural network structure and/or by enlarging the size of experimental data and regression model by removing non-significant terms from (Eq. 4).The variation in Nash-Scutcliffe efficiency (NSE), root means square error (RMSE) and a mean square absolute error (MAE) value presented in Table 8 validate the excellent forecasting ability of the developed models.

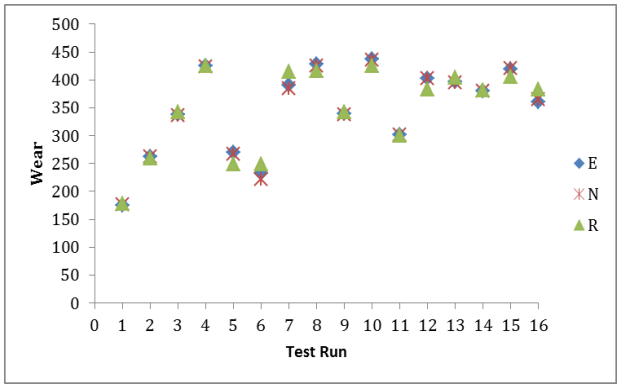

Fig. 8. Experimental and predicted wear values.

Table 8. Statistical pointer for model.

Test	ANN Model			Regression Model		
	RSME	**MAE**	**NSE**	**RSME**	**MAE**	**NSE**
1	0.38	-0.046	1.00	0.70	0.039	1.00
2	0.17	0.062	1.00	0.47	0.052	1.00
3	0.33	-0.107	0.98	1.13	0.041	0.77
4	0.33	-0.017	1.00	0.03	0.042	1.00
5	0.83	0.422	1.00	5.40	0.011	0.92
6	2.38	-0.719	0.99	4.30	-0.086	0.98
7	1.38	-0.487	0.98	6.22	-0.024	0.66
8	0.75	0.139	1.00	3.13	0.016	0.98
9	0.25	-0.088	0.99	0.95	0.046	0.79
10	0.17	0.149	1.00	2.78	0.052	0.98
11	0.00	0.053	1.00	0.63	0.063	1.00
12	0.00	0.314	1.00	5.08	0.063	0.87
13	0.08	-0.124	1.00	1.88	0.058	0.98
14	0.08	-0.027	1.00	0.50	0.058	1.00
15	0.25	0.224	1.00	3.50	0.047	0.96
16	0.00	-0.317	0.91	5.58	0.057	-1.65

4. CONCLUSIONS

The following are the conclusions drawn from this study:

1. The stir casting process is successfully implemented for the fabrication of hybrid composite based on aluminum zinc alloy with graphite and SiC.
2. The least porosity, utmost tensile strength, least wear rate and comparable hardness is noticed for the material with 10 wt.% of SiC and 3 wt.% of graphite indicates the outstanding bonding strength and chemical solubility among SiC, graphite and matrix alloy. However, tensile strength, hardness and wear resistance decreases with further rise of SiC, owing to reduction in bonding strength and solid solubility and that leads to rise in porosity.
3. ANN and regression model developed models are found precise for the forecasting of wear characteristics of the manufactured materials. Confirmation test yield small error in predicted and experimental wear value validate that the derived model is precisely capable for forecasting the wear characteristics of material.
4. The temperature is most contributing factor with of 46.88 %, followed by load (28.30 %), sliding speed (20.36 %), percentage reinforcement (0.706 %) and sliding distance (0.7 %).
5. The abrasion, adhesion and delamination wear mechanism is noticed from SEM micrographs. For the high value of operating parameters material with 0, 20 and 30 wt.% of SiC experience severe wear. Whereas, the material with 10 wt.% of SiC undergoes mild wear.

Acknowledgement

The author would like thanks BCUD Savitribai Phule Pune University for providing finance for this Research work: 15ENG002473.

REFERENCES

[1] B.K. Prasad, A.H. Yegneswaran, A.K. Patwardhan, *Influence of the nature of micro constituents on the*

tensile properties of a zinc-based alloy and a leaded-tin bronze at different strain rates and temperatures, Journal of material science, vol. 32, iss. 5, pp. 1169–1175, 1997, doi: 10.1023/A:1018523732492

[2] B.K. Prasad, A.K. Patwardhan, A.H. Yegneswaran, *Microstructure and Property Characterization of a Modified Zinc-Base Alloy and Comparison with Bearing Alloys*, Journal of Materials Engineering and Performance, vol. 7, iss. 1, pp. 130-135, 1998, doi: 10.1361/105994998770348151

[3] B.K. Prasad, S. Das, O.P. Modi, A.K. Jha, R. Dasgupta, A.H. Yegneswaran, *Wear Response of a Zn-Base Alloy in the Presence of Sic Particle Reinforcement: A Comparative Study with a Copper-Base Alloy*, Journal of Materials Engineering and Performance, vol. 8, iss. 6, pp. 693-700, 1999, doi: 10.1361/105994999770346468

[4] G. Purcek, T. Savaskan, T. Kucukomeroglu, S. Murphy, *Dry sliding friction and wear properties of zinc-based alloys,* Wear, vol. 252, iss. 11-12, pp. 894–901, 2002, doi: 10.1016/S0043-1648(02)00050-9

[5] T. Savaskan, A.P. Hekimoglu, G. Purcek, *Effect of copper content on the mechanical and sliding wear properties of monotectoid-based zinc-aluminium-copper alloys,* Tribology International, vol. 37, iss. 1, pp. 45–50, 2004, doi: 10.1016/S0301-679X(03)00113-0

[6] B.K. Prasad, *Dry sliding wear response of zinc-based alloy over a range of test speeds and loads: a comparative study with cast iron*, Tribology Letters, vol. 25, iss. 2, pp. 103-115, 2007, doi: 10. 1007/s11249-006-9054-3

[7] T. Savaskan, Z. Azakli, *An investigation of lubricated friction and wear properties of Zn–40Al–2Cu–2Si alloy in comparison with SAE 65 bearing bronze,* Wear, vol. 264, iss. 11-12, pp. 920–928, 2008, doi: 10.1016/j.wear.2007.06.008

[8] M. Babic, S. Mitrovic, B. Jeremic, *The influence of heat treatment on the sliding wears behaviour of a ZA-27 alloy,* Tribology International, vol. 43, iss. 1-2, pp. 16–20, 2010, doi: 10.1016/j.triboint.2009.04.016

[9] Y. Alemdag, T. Savaskan, *Mechanical and tribological properties of Al– 40Zn–Cu alloys*, Tribology International, vol. 42, iss. 1, pp. 176–182, 2009, doi: 10.1016/j.triboint.2008.04.008

[10] T. Savaskan, O. Bican, Y. Alemdag, *Developing aluminium–zinc-based a new alloy for tribological applications,* Journal of Materials Science, vol. 44, iss. 8, pp. 1969–1976, 2009, doi: 10.1007/s10853-009-3297-y

[11] C. Perrin, P.A. Shenton, Dana Corporation, *Aluminium alloy and method for production thereof*, Patent No. WO 01/34330 Al, 2001.

[12] H.S. Kang, Hyundai Motor Company, Seoul (Kr), *Wear resistant alloy having complex microstructure*, Application No. 14/270,674, Patent No. US2014/0334970Al, 2014.

[13] T. Savaskan, H.O. Tan, *Fatigue behaviour of Al-25Zn-3Cu alloy,* Materials Science and Technology, vol. 30, iss. 8, pp. 938-943, 2014, doi: 10.1179/1743284713Y.0000000362

[14] O. Bican, T. Savaskan, *A comparative study of lubricated friction and wear behaviour of AL-25Zn-3Cu-3Si bearing alloy*, Proceedings of the Institution of Mechanical Engineers, Part J: Journal of Engineering Tribology, vol. 228, iss. 8, pp. 896-903, 2014, doi: 10.1177/1350650114537473

[15] O. Bican, T. Savaskan, *Influence of Test Conditions on the Lubricated friction and wear behaviour of Al–25Zn–3Cu Alloy*, Tribology Letter, vol. 37, iss. 2, pp. 175–182, 2010, doi: 10.1007/s11249-009-9509-4

[16] T. Savaskan, O. Bican, *Dry sliding friction and wear properties of Al–25Zn– 3Cu–3Si alloy,"* Tribology International, vol. 43, iss. 8, pp. 1346–1352, 2010, doi: 10.1016/j.triboint.2010.01.001

[17] T. Savaskan, O. Bican, *Dry Sliding Friction and Wear Properties of Al–25Zn–3Cu–(0–5) Si Alloys in the As-Cast and Heat-Treated Conditions,* Tribology Letter, vol. 40, iss. 3, pp. 327-336, 2010, doi: 10.1007/s11249-010-9667-4

[18] S.C. Sharma, B.M. Girish, D.R. Somashekar, R. Kamath, B.M. Satish, *Mechanical properties and fractography of zircon particle reinforced ZA-27alloy composite materials*, Composite science and technology, vol. 59, iss. 12, pp. 1805-1812, 1999, doi: 10.1016/S0266-3538(99)00040-8

[19] G. Ranganath, S.C. Sharma, M. Krishna, *Dry sliding wear of garnet reinforced zinc/aluminium metal matrix composites,* Wear, vol. 251, iss. 1-12, pp. 1408–1413, 2001, doi: 10.1016/S0043-1648(01)00781-5

[20] S.C. Sharma, K.H.W. Seah, B.M. Satish, B.M. Girish, *Effect of short glass fibers on the mechanical properties of cast ZA-27 alloy composites,* Materials & Design, vol. 17, iss. 5-6, pp. 245-250, 1996, doi: 10.1016/S0261-3069(97)00016-2

[21] S.C. Sharma, B.M. Girish, B.M. Satish, R. Kamath *Aging Characteristics of Short Glass Fiber Reinforced ZA-27Alloy Composite Materials*, Journal of Materials Engineering and Performance, vol. 7, iss. 6, pp. 747-750, 1998, doi: 10.1361/105994998770347305

[22] S.C. Sharma, *Elastic Properties of Short Glass Fiber-Reinforced ZA-27 Alloy Metal Matrix Composites,* Journal of Materials Engineering and Performance, vol. 10, iss. 4, pp. 468–474, 2001, doi: 10.1361/105994901770344908

[23] M. Babic, S. Mitrovic, F. Zivic, I. Bobic, *Wear behaviour of composites based on ZA-27 based composites reinforced with Al2O3 particles under dry sliding condition,* Tribology Letters, vol. 38, iss. 3, pp. 337-346, 2010, doi: 10.1007/s11249-010-9613-5

[24] G. Ranganath, S.C. Sharma, M. Krishna, M.S. Muruli, *A Study of Mechanical Properties and Fractography of ZA-27/Titanium-Dioxide Metal Matrix Composites*, Journal of Materials Engineering and Performance, vol. 11, iss. 4, pp. 408-13, 2002, doi: 10.1361/105994902770343935

[25] S. Baskaran, V. Anandakrishnan, M. Duraiselvam, *Investigation on dry sliding wear behaviour of in situ casted AA7075-TiC metal matrix composites by using Taguchi's technique*, Materials & Design, vol. 60, pp. 184-192, 2014, doi: 10.1016/j.matdes.2014.03.074

[26] K.H.W Seah, S.C. Sharma, B.M. Girish, *Mechanical properties of as-cast and heat-treated ZA-27/graphite particles composites*, Composites Part A: Applied Science and Manufacturing, vol. 28, iss. 3, pp. 251-256, 1997, doi: 10.1016/S1359-835X(96)00117-0

[27] K.H.W Seah, S.C. Sharma, B.M. Girish, *Mechanical properties of cast ZA27-graphite particles composites, Materials and Design,* vol. 16, iss. 5, pp. 271-275, 1995, doi: 10.1016/0261-3069(96)00001-5

[28] M. Babic, M. Slobodan, D. Dzunic, B. Jeremic, I. Bobic, *Tribological behaviour of composites based on ZA-27 alloy reinforced with graphite particles,* Tribology Letters, vol. 37, iss. 2, pp. 401-410, 2010, doi: 10.1007/s11249-009-9535-2

[29] A. Baradeswaran, A.E. Perumal, *Study on mechanical and wear properties of Al7075/Al_2O_3/graphite hybrid composites*, Composites Part B: Engineering, vol. 56, pp. 464-471, 2014, doi: 10.1016/j.compositesb.2013.08.013

[30] S.C. Sharma, B.M. Girish, R. Kamath, B.M. Satish, *Effect of SiC particle reinforcement on the unlubricated sliding wear behaviour of ZA-27 alloy composites*, Wear, vol. 213, iss. 1-2, pp. 33-40, 1997, doi.org/10.1016/S0043-1648(97)00185-3

[31] S.C. Tjong, F. Chen, *Wear Behaviour of As-Cast ZnAl27 /SiC Particles Metal-Matrix Composites under Lubricated Sliding Condition*, Metallurgical and Materials Transactions A, vol. 28, iss. 9, pp. 1951-55, 1997, doi: 10.1007/s11661-997-0127-1

[32] B. Stojanovic, M. Babic, S. Mitrovic, A. Vencl, N. Miloradovic, M. Pantic, *Tribological Characteristics of Aluminium Hybrid Composites Reinforced With SiC and Graphite. A Review,* Journal of the Balkan Tribological Association, vol. 19, pp. 83–96, 2013.

[33] R.N. Rao, S. Das, *Effect of matrix alloy and influence of SiC particle on the sliding wear characteristics of aluminium alloy composites*, Material & Design, vol. 31, iss. 3, pp. 1200-1207, 2010, doi: 10.1016/j.matdes.2009.09.032

[34] S.K. Ghosh, P. Saha, Crack *and wear behavior of SiC particulate reinforced aluminium based metal matrix composite fabricated by direct metal laser sintering process*, Material & Design, vol. 32, iss. 1, pp. 139-145, 2011, doi: 10.1016/j.matdes.2010.06.020

[35] T.B. Rao, *An experimental investigation on mechanical and wear properties of Al7075/SiCp composites: effect of SiC content and particle size*, Journal of Tribology, vol. 140, iss. 3, p. 8, 2017, doi: 10.1115/1.4037845

[36] S.S. Mahapatra, A. Patnaik, *Study on mechanical and erosion wear behaviour of hybrid composites using Taguchi experimental design*," Materials and Design, vol. 30, iss. 8, pp. 2791–2801, 2009, doi: 10.1016/j.matdes.2009.01.037

[37] P.R. Pati, A. Satapathy, *Triboperformance analysis of coating of LD slag premixed with TiO2 using experimental design and ANN*, Tribology Transactions, vol. 58, iss. 2, pp. 349-356, 2015, doi: 10.1080/10402004.2014.971995

[38] T. Thankachan, K.S. Prakash, M. Kamarthin, *Optimizing the tribological behavior of hybrid copper surface composite using statistical and machine learning techniques*, Journal of Tribology, vol. 140, iss. 3, p. 8, 2018, doi: 10.1115/1.4038688

[39] G. Villarrubia, J.F. De Paz, P. Chamoso, F. De la Prieta, *Artificial neural networks used in optimization problems,* Neurocompouting, vol. 272, pp. 10-16, 2018, doi: 10.1016/j.neucom.2017.04.075

[40] J. Hasim, L. Looney, M.S.J. Hashim, *The enhancement of wettability of SiC particles in cast aluminium matrix composites,* Journals of Material Processing Technology, vol. 119, iss. 1-3, pp. 329-335, 2001, doi: 10.1016/S0924-0136(01)00919-0

[41] R. Mitra, V.S.C. Rao, R. Maiti, M. Chakraborty, *Stability and response to rolling of the interfaces in cast Al-SiCp and Al-mg-SiCp composites*, Materials science and Engineering: A, vol. 379, iss. 1-2, pp. 391-400, 2004, doi: 10.1016/j.msea.2004.03.024

[42] R. Ramesh, R. Gnanamoorthy, *Fretting wear behavior of liquid nitrided structural steel En24 and bearing steel, En31,* Journal of Materials Processing Technology, vol. 171, iss. 1, pp. 61-67, 2006, doi: 10.1016/j.jmatprotec.2005.06.048

[43] M.S. Charoo, M.F. Wani, M. Hanief, A. Chetani, M.A. Rather, *Tribological characteristics of EN8 and EN24 Steel against aluminium alloy 6061 under lubricated condition,* advanced material Proceedings, vol. 2, no. 7, pp. 445-449, 2017, doi: 10.5185/amp.2017/709

[44] C.R. Rao, M. Statistiker, *Linear statistical inference and its applications*, New York: Wiley, 1973.

[45] P.P. Ritapure, Y.R. Kharde, *Effect of Graphite Addition on Mechanical Properties and Elevated Temperature Tribological Behaviour of Aluminium Zinc Alloy,* in 2nd International Conference on Tribology, TRIBOINDIA-2018, 13th -15th December 2018, VJTI, Mumbai, India.

[46] P. Gupta, D. Kumar, A.K. Jha, O.M. Parkash, *Effect of height to diameter (h/d) ratio on the deformation behaviour Fe-Al_2O_3 metal matrix nanocomposites,* Bulletin of Material Science, vol. 39, iss. 5, pp. 1245–1258, 2016, doi: 10.1007/s12034-016-1272-1

[47] P. Gupta, D. Kumar, O. Parkash, A.K. Jha, K.K. Sadasivuni, *Dependence of Wear Behavior on Sintering Mechanism for Iron-Alumina Metal Matrix Nanocomposites*, Materials Chemistry and Physics, vol. 220, pp. 441-448, 2018, doi: 10.1016/j.matchemphys.2018.08.079

[48] P. Gupta, D. Kumar, O. Parkash, A.K. Jha, *Effect of sintering on wear characteristics of Fe-Al_2O_3 metal matrix composites,* Proceedings of the Institution of Mechanical Engineers, Part J: Journal of Engineering Tribology, vol. 228, iss. 3, pp. 362-368, 2017 doi: 10.1177/1350650113508934

[49] P. Garg, P. Gupta, D. Kumar, O. Parkash, *Structural and Mechanical Properties of Graphene reinforced Aluminum Matrix Composites*, Journal of Material Environmental Science, vol. 7, no. 5, pp. 1461-1473, 2016.

[50] U.J.P. Kumar, P. Gupta, A.K. Jha, D. Kumar, *Closed die deformation behaviour of cylindrical Iron-Alumina metal matrix composites during cold sinter forging,* Journal of Institute of Engineers (India): series D, vol. 98, iss. 1, pp. 135-151, 2016, doi: 10.1007/s40033-015-0089-1